

DuoTok: Source-Aware Dual-Track Tokenization for Multi-Track Music Language Modeling

Rui Lin* Zhiyue Wu* Jiahe Lei Kangdi Wang Weixiong Chen

Junyu Dai^{§†} Tao Jiang

εar-lab, initi:AI Ltd

*Equal Contribution §Corresponding Author †Project Lead

Abstract

Audio tokenization is the interface between continuous waveforms and multi-track music language models. In the dual-track setting, tokens should support high-fidelity reconstruction, be predictable under a Language Model (LM), and preserve cross-track correspondence. We propose DuoTok, a dual-track music tokenizer that resolves this tension via *staged disentanglement*. DuoTok pretrains a semantic encoder, structurally regularizes it with multi-task supervision, then freezes the encoder and applies hard dual-codebook routing while retaining auxiliary objectives on *quantized* codes. A diffusion decoder reconstructs high-frequency details so the tokens can focus on structured information for sequence modeling.

On standard benchmarks, DuoTok achieves a favorable predictability–fidelity trade-off, attaining the lowest cnBPT while maintaining competitive reconstruction at 0.75 kbps. On a held-constant dual-track LM protocol, enBPT also improves, indicating gains beyond codebook-size effects. Controlled diagnostics further show larger predictability costs under cross-track corruption and larger gains from longer context, supporting that LMs trained on DuoTok tokens leverage cross-track structure and non-local history.

1 Introduction

Recent generative music systems increasingly adopt multi-track language models over discrete audio tokens (Yuan et al., 2025; Lei et al., 2025). By modeling vocals and accompaniment as synchronized streams, they enable controllable and editable generation, while also allowing training to better leverage large speech corpora for vocals and broad background music (BGM) / instrumental music corpora for accompaniment. In this paradigm, the audio tokenizer is more than a compression module. It is the **interface** between continuous

waveforms and sequence modeling, jointly determining reconstruction fidelity and the modelability of token sequences under an LM.

Yet existing tokenizers remain misaligned with the requirements of multi-track language modeling. Reconstruction-oriented neural codecs such as EnCodec and DAC prioritize waveform fidelity, but preserve abundant fine-grained acoustic variability. Their token sequences are therefore difficult to model (Défossez et al., 2022; Ji et al., 2024; Kumar et al., 2023). Semantic-oriented tokenizers aim for LM-friendly representations, but often sacrifice the spectral precision needed for high-quality music reconstruction (Liu et al., 2024; Zhang et al., 2024; Ye et al., 2024). Moreover, overly aggressive quantization can erode high-level musical attributes (e.g., genre and mood), which directly limits controllable generation. More fundamentally, many tokenizers are *structure-blind* in the multi-track setting. Shared codebooks can entangle vocal and accompaniment information, while fully independent token spaces weaken the inductive bias for cross-track correspondence. This creates a central dilemma: how can we isolate tracks for editing without severing their logical dependency?

We propose DuoTok, a dual-track music tokenizer designed to be LM-friendly without abandoning reconstruction quality. Our core idea is *staged disentanglement*. We first encourage source-aware structure in the continuous space, and then discretize with hard dual-codebook routing. This ordering lets the routing step build on an encoder that already reflects cross-track alignment, promoting physical separation without sacrificing learned correspondence.

Concretely, DuoTok firstly builds a general semantic representation foundation via self-supervised pretraining in Stage 1. In Stage 2, we apply feature replacement noise to encourage context-level semantic consistency, and introduce two auxiliary heads—MSS (Music Source Separation) and

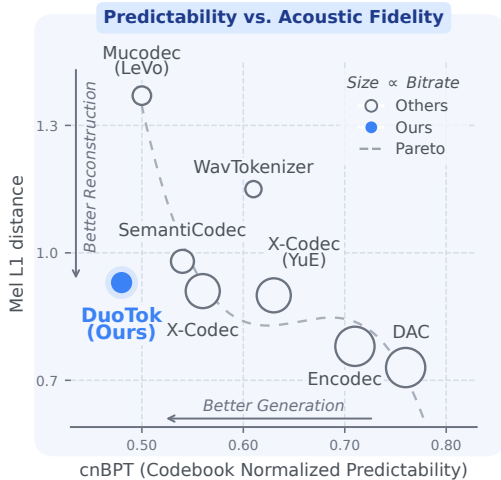


Figure 1: **Predictability vs. acoustic fidelity.** Bubble size denotes bitrate. DuoTok (blue) achieves the lowest cnBPT while maintaining competitive Mel distance compared to baselines, indicating an improved trade-off between LM modelability and reconstruction quality.

an ASR (Automatic speech recognition) head for lyric alignment—in addition to spectrum-field reconstructions like Mel and Chroma, encouraging source separation and semantic alignment in the continuous space (Song et al., 2025; Défossez et al., 2019). This regularization prepares the encoder for Stage 3, where we freeze the encoder and discretize with hard dual-codebook routing. We retain auxiliary heads in the discretization training so that separation and alignment objectives shape the discrete token space. Empirically, with the two streams pre-aligned in the continuous space, hard routing reduces physical interference while retaining learned correspondence, as supported by the corruption sensitivity in Fig. 3 and the context-scaling results in Fig. 4. Finally, a diffusion decoder reconstructs high-frequency details, allowing the discrete tokens to focus on structured information that benefits sequence modeling.

Our main contributions are:

- **Staged disentanglement for dual-track tokenization.** We propose DuoTok, a dual-track tokenizer instantiated by a staged disentanglement recipe. DuoTok learns a physically separable token space with a frozen encoder before discretization and retains auxiliary objectives during discretization training, thereby facilitating cross-track synchronization and correspondence for multi-track LMs.
- **A better predictability–fidelity operating**

point. We visualized in Fig. 1 that DuoTok achieves the lowest cnBPT among compared methods while maintaining competitive reconstruction quality at ultra-low bitrate.

- **Controlled diagnostics for cross-track structure.** We introduce controlled perturbation analyses that quantify the predictability cost of cross-track corruption (Fig. 3) and the benefits of longer context (Fig. 4). These diagnostics show that DuoTok yields stronger structural modeling capabilities and larger long-context gains than baselines.

2 Related Work

Audio tokenizers for generative modeling. Discrete audio tokenizers define the sequences that language models must predict, so the tokenizer objective directly determines the difficulty of LM modeling. Reconstruction-oriented neural codecs such as SoundStream (Zeghidour et al., 2021), EnCodec (Défossez et al., 2022), DAC (Kumar et al., 2023) and WavTokenizer (Ji et al., 2024) prioritize perceptual fidelity and bitrate efficiency. However, their acoustic tokens preserve substantial fine-grained variability, which impedes effective modeling of long-range sequences. Conversely, Self-supervised models adopt a different approach by prioritizing high-level latent features. For instance, masked prediction in wav2vec 2.0 (Baevski et al., 2020), HuBERT (Hsu et al., 2021), and WavLM (Chen et al., 2021) learns robust latent structures, while BEST-RQ-style discretization (Baumann et al., 2025) provides efficient targets for this objective. Since purely semantic representations are lossy for music as they discard essential timbre and texture cues, recent tokenizers including SemanticCodec (Liu et al., 2024) and SpeechTokenizer (Zhang et al., 2024) integrate SSL priors into codec-style discretization to bridge the gap between predictability and fidelity. This hybrid approach also extends to conflict-mitigating designs (Gong et al., 2024) and streaming systems employing distilled semantic guidance (Défossez et al., 2024; Ye et al., 2024). Despite this progress, most tokenizers remain optimized for single-stream or mixture-centric objectives, and cross-track correspondence is rarely treated as a first-class constraint in the discrete token space.

Multi-track music generation with discrete LMs. Token-based music generation commonly

follows a tokenizer-LM-renderer pipeline. Early model-scaling-driven music generation systems, such as MusicLM (Agostinelli et al., 2023) and SongGen (Liu et al., 2025), typically adopt a single-stream modeling approach. However, this paradigm fails to account for the disparity in information density and fine-grained editing requirements between vocals and accompaniment. Such challenges motivate multi-track LMs that model synchronized streams to provide superior controllability. Recent advances, including YuE (Yuan et al., 2025) and SongCreator (Lei et al., 2024), and the preference-aligned LeVo (Lei et al., 2025), adopt explicit dual-track modeling to improve performance. Other approaches, such as SongBloom (Yang et al., 2025), combine autoregressive sketching with refinement modules. Although these structured objectives improve controllability, they reveal an underlying representational bottleneck. This motivates structure-aware tokenization that jointly optimizes LM predictability, reconstruction fidelity, and cross-track correspondence. Accordingly, we evaluate LM predictability in a held-constant dual-track setting for tokenizers paired with established multi-track pipelines, and benchmark our results against a broader family of representative codecs.

3 DuoTok

Overview. DuoTok is a dual-track music tokenizer that serves as a *sequence modeling interface* between raw audio and multi-track language models (Yuan et al., 2025; Lei et al., 2025). By discretizing separated vocal and accompaniment stems into time-aligned latent streams, DuoTok facilitates flexible modeling paradigms, including unconditional and track-conditioned synthesis. The training process comprises four stages in Figure 2: Stage 1 semantic pretraining, Stage 2 structurally-regularized acoustic adaptation, Stage 3 dual-track discretization, and Stage 4 high-fidelity diffusion decoding (Rombach et al., 2022; Peebles and Xie, 2022). To ensure practical applicability, we rely on pseudo-stems obtained through off-the-shelf separation tools (Défossez et al. (2019), Lu et al. (2023)) instead of ground-truth sources. Full hyperparameters are provided in Appendix C.

Design objectives. Our design is guided by three objectives aligned with our evaluation axes:

- **Predictability:** tokens should be easy to

model under multi-track LMs, including cross-track conditioning.

- **Semantic preservation:** tokens should retain high-level musical attributes and track structure.
- **Reconstruction fidelity:** tokens should remain decodable with sufficient spectral detail.

3.1 Stage 1 Semantic pretraining

Stage 1 learns a high-level audio representation with self-supervised pretraining (Baevski et al., 2020; Hsu et al., 2021; Chen et al., 2021). To provide a semantic foundation that is well-suited for subsequent tokenization, we adopt BEST-RQ to encourage content-oriented discrete targets (Bauermann et al., 2025). This allows later stages to progressively adapt this representation toward precise waveform reconstruction.

3.2 Stage 2 Acoustic adaptation with structural regularization

To bridge the predictability-reconstruction gap in Stage 1, **Stage 2** performs *acoustic adaptation* by imposing *structural regularization* via feature replacement noise and auxiliary supervision (Song et al., 2025). This strategy prevents the representation from collapsing into low-level acoustic patterns, thereby preserving the global learnability established in the pretraining phase.

Feature replacement noise. Given hidden features $\mathbf{h}_{1:T}$, we stochastically replace a subset of time steps with Gaussian noise:

$$\begin{aligned}\tilde{\mathbf{h}}_t &= (1 - m_t)\mathbf{h}_t + m_t\boldsymbol{\epsilon}_t, \\ \boldsymbol{\epsilon}_t &\sim \mathcal{N}(\mathbf{0}, \sigma^2\mathbf{I}),\end{aligned}\tag{1}$$

where m_t is a Bernoulli mask and σ is estimated from feature statistics (Song et al., 2025).

Optimization objective. We optimize a weighted sum of acoustic losses and structural regularizers:

$$\mathcal{L}^{(2)} = \underbrace{\mathcal{L}_{\text{mel}} + \lambda_{\text{chr}}\mathcal{L}_{\text{chr}}}_{\text{Acoustic}} + \underbrace{\lambda_{\text{asr}}\mathcal{L}_{\text{asr}} + \lambda_{\text{mss}}\mathcal{L}_{\text{mss}}}_{\text{Structural}}.\tag{2}$$

Here \mathcal{L}_{mel} and \mathcal{L}_{chr} recover spectral details, and \mathcal{L}_{asr} provides text-aligned supervision through an ASR head for lyric alignment.

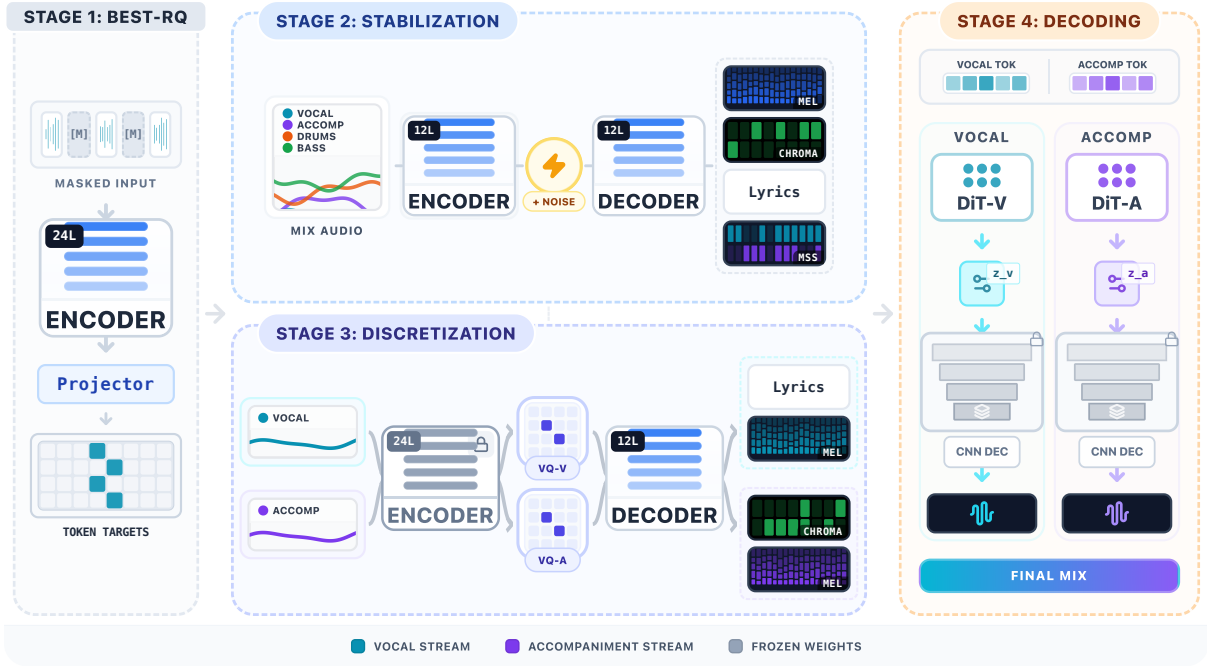


Figure 2: **DuoTok pipeline.** Stage 1 provides a semantic representation. Stage 2 performs acoustic adaptation with structural regularization. Stage 3 learns dual-track discretization with track-aware routing and dual codebooks. Stage 4 employs diffusion decoders for waveform reconstruction.

MSS supervision via mask distillation. Rather than regressing separated waveforms, we distill multi-source MSS structure from a frozen separator (Lu et al., 2023; Rafi et al., 2019). The teacher predicts a set of soft time–frequency masks $\{M^{(s)}\}_{s=1}^K$, and our MSS head predicts $\{\hat{M}^{(s)}\}_{s=1}^K$ from encoder features. We match masks with

$$\mathcal{L}_{\text{mss}} = \sum_{s=1}^K \left\| \hat{M}^{(s)} - M^{(s)} \right\|_1. \quad (3)$$

Mask distillation provides source-aware structural cues while reducing the risk that separation artifacts directly corrupt the representation, which stabilizes later discretization.

3.3 Stage 3 Dual-track discretization with routing

The first two stages learn a continuous representation that balances semantic content, acoustic detail, and track-aware structure. **Stage 3** then *discretizes* this representation into dual-track token streams; we freeze the encoder to preserve the learned structure while training the quantizers. Given a track indicator $r \in \{\text{vocal}, \text{accompaniment}\}$, we route features to a track-specific quantizer with codebook \mathcal{C}_r . To enhance utilization and stability, we adopt a linear-reparameterized SimVQ with a basis W_r

and quantize in the transformed space $\tilde{\mathcal{C}}_r = \mathcal{C}_r W_r$:

$$k_t = \arg \min_j \|\mathbf{h}_t - \tilde{\mathbf{c}}_j^{(r)}\|_2^2, \quad \mathbf{q}_t = \tilde{\mathbf{c}}_{k_t}^{(r)}. \quad (4)$$

A straight-through estimator minimizes the VQ commitment loss \mathcal{L}_{vq} alongside auxiliary objectives (Zhu et al., 2024).

Auxiliary heads on quantized representations. We retain the reconstruction and alignment heads from Stage 2 on the *quantized* representation \mathbf{q}_t . In Stage 3, inputs are track-separated pseudo-stems, so MSS mask supervision is not activated. Keeping the remaining heads on quantized codes makes the objectives act directly on the discrete token space. The objective is:

$$\mathcal{L}^{(3)} = \mathcal{L}_{\text{mel}} + \lambda_{\text{chr}} \mathcal{L}_{\text{chr}} + \lambda_{\text{asr}} \mathcal{L}_{\text{asr}} + \lambda_{\text{vq}} \mathcal{L}_{\text{vq}}. \quad (5)$$

3.4 Stage 4 Latent diffusion decoding

Stage 4 decouples macro-structure from fine-detail synthesis by reconstructing each track with a latent diffusion decoder. Conditioned on Stage 3 tokens, this decoder predicts pre-trained ear-VAE latents (Wang et al., 2025a), shifting the burden of micro-acoustic generation to a dedicated renderer. This modular design further facilitates a *matched-decoder evaluation*: by training a standardized decoder on various frozen codebooks, we can directly

probe the intrinsic reconstructability of the tokens while minimizing decoder-related confounding factors.

4 Experiments

4.1 Setup

Data and preprocessing. DuoTok is trained exclusively on public corpora. Stage 1 uses a broad mixture of speech, general audio, and music, while Stage 2–Stage 4 focus on music and vocal-centric content. To enable dual-track learning without proprietary stems, we synthesize pseudo vocal and accompaniment stems using Demucs (Défossez et al., 2019). We segment audio into 5–30s clips, when lyrics are available, we apply lyric-aware segmentation aligned to sentence boundaries. Comprehensive details regarding dataset splits and preprocessing are in Appendix C.

Supervision and alignment. For lyric alignment, we attach an ASR head with the bert-base-multilingual-cased tokenizer (Devlin et al., 2018) to provide timing supervision for lyrics. Chinese and English lyric transcripts are generated with WhisperX and FunASR (Bain et al., 2023; Gao et al., 2023). This lyric supervision is applied in 5/7 of Stage 2 updates and in roughly half of Stage 3 updates; detailed data categories and sampling ratios are in Appendix C.2.

For MSS regularization, we additionally distill music source separation supervision from a frozen BS-RoFormer teacher (Lu et al., 2023), which predicts soft time–frequency masks for four MUSDB-style stems (vocals, drums, bass, and other).

Baselines. We compare against representative tokenizers from three families: reconstruction-oriented neural codecs, semantic-oriented tokenizers, and music-oriented tokenizers used in recent multi-track generation systems. We use official checkpoints and default configurations whenever available.

Training overview and compute budget. We train DuoTok in four stages using AdamW with a warmup–cosine schedule, on 64 NVIDIA A100 GPUs. Stage 1 runs for 3M steps (~5 days), Stage 2 for 100k steps (~6 days) with BS-RoFormer teacher supervision, and Stage 3 for 100k steps (~2 days) with the MSS head removed. Comprehensive hyperparameters, loss weights, and implementation details are in Appendix C.

4.2 Evaluation protocols

We evaluate tokenizers applying standardized and auditable procedures with held-constant settings. Details are deferred to Appendix B.1 for LM evaluation, Appendix B.2 for probing, and Appendix B.3.1–B.4 for matched decoder and MOS.

Multi-track LM protocol. Across all tokenizers, we train the same Qwen2-1B backbone under identical optimizer and schedule, total optimization steps, and 30 s audio context. We evaluate both **parallel prediction** and **track-to-track conditioning**. Multi-codebook input formatting, loss computation, and auxiliary metrics are provided in Appendix B.1.

Tagging probe protocol. We freeze each tokenizer and train a lightweight probe only on post-quantization codebook embeddings for MagnaTagATune Top-50, reporting Average Precision(AP) and Area Under the Curve(AUC). Probe architecture and training details are in Appendix B.2.

Reconstruction protocol. We report each tokenizer’s native reconstruction pipeline. We additionally perform a matched-decoder comparison by training the same latent diffusion decoder on frozen codebook embeddings for DuoTok and MuCodec to predict ear-VAE latents, and verify perceptual quality via a blinded MOS study. Settings are in Appendix B.3.1 and Appendix B.4.

4.3 Metrics

We evaluate tokenizers primarily by downstream modeling performance and reconstruction quality, with additional metrics reported where relevant.

Predictability. We measure token-level cross-entropy in bits per token (BPT), $BPT = \log_2 PPL$. Because BPT scales with codebook size S , we report the codebook-normalized metric

$$cnBPT = \frac{BPT}{\log_2 S}, \quad (6)$$

which measures coding efficiency relative to fixed-length index coding. Derivations and the multi-codebook extension are in Appendix A.1.

When the empirical code distribution is reliably estimable (our held-constant dual-track LM benchmark), we additionally report entropy-normalized BPT:

$$enBPT = \frac{BPT}{H(p)}, \quad (7)$$

where $H(p)$ is the empirical unigram entropy on the evaluation set (Appendix E.1). Unlike cnBPT, enBPT removes the uniform-code assumption, but consistent $H(p)$ estimation is not available for all tokenizers; hence we use cnBPT as the unified metric and reserve enBPT for that benchmark. Since tokenizers also differ in token rate τ , we report a per-second normalized metric (cnBPS) in Appendix A.3.

Musical attribute preservation. We assess whether post-quantization codes preserve high-level musical concepts via MagnaTagATune Top-50 multi-label tagging (Law et al., 2009), reporting Average Precision and AUC.

Reconstruction. We quantify the reconstruction fidelity with Mel distance, supplemented by speech-centric perceptual metrics including PESQ and STOI. In matched-decoder scenarios, we extend the evaluation to include subjective Mean Opinion Scores (MOS) on a 1–5 scale to better capture human auditory preferences (Appendix B.3.1 and Appendix B.4).

5 Main Results

5.1 Modeling-Reconstruction Balance

Fig. 1 illustrates the optimization dilemma between cnBPT and Mel distance, revealing the performance gap between reconstruction-heavy codecs (Défossez et al., 2022; Ji et al., 2024; Kumar et al., 2023) and semantic tokenizers (Liu et al., 2024; Ye et al., 2024). Within this landscape, DuoTok achieves the minimum cnBPT without sacrificing reconstruction fidelity (Table 1). Compared to MuCodec (LeVo) at similar bitrates (Lei et al., 2025), DuoTok provides simultaneous improvements in both metrics. This suggests that the proposed architecture reduces the coupling between modeling complexity from acoustic fidelity, thereby avoiding the fidelity degradation prevalent in existing models.

5.2 Multi-track Parallel LM Predictability

We evaluate predictability of discrete representations under the held-constant protocol in Sec. 4.2. To quantify modeling complexity, we report cnBPT alongside enBPT, which accounts for the empirical unigram code entropy estimated on the evaluation set (Appendix E.1).

Unconditional Generation. As shown in Table 2, DuoTok achieves the lowest average cnBPT

(**0.483**), significantly improving over X-Codec in YuE (0.631) and MuCodec in LeVo (0.501). Under the stricter enBPT metric, DuoTok performs on par with MuCodec in LeVo (0.516) and substantially outperforms X-Codec in YuE (0.754). Similarly, DuoTok maintains competitive Top-k accuracy ($\text{Acc}@k$), demonstrating robust sequence modeling capabilities despite the challenges posed by its larger vocabulary size.

Track-to-track LM Predictability. The model’s ability to capture cross-track dependencies is evaluated through vocal-conditioned accompaniment generation (Table 3). DuoTok achieves the lowest BPT across both normalization schemes (**0.464** for cnBPT and **0.489** for enBPT respectively), indicating a superior capacity for capturing cross-track dependency. To further isolate the impact of this cross-track synchronization, controlled sensitivity analyses are conducted in Sec. 6.1.

5.3 Musical Attribute Preservation via Tagging

We evaluate the preservation of musical attributes through the MTT multi-label tagging benchmark. As detailed in Table 1, a probe trained on frozen post-quantization embeddings achieves AP of 0.35 and AUC of 0.87 for DuoTok. This robust attribute preservation under ultra-low bitrates suggests that DuoTok effectively captures semantic features essential for musical understanding and controllable generation.

5.4 Matched-Decoder Reconstruction

To eliminate performance discrepancies stemming from disparate decoder designs, we evaluate DuoTok and MuCodec (LeVo) under a unified decoder framework (Appendix B.3.1). As shown in Table 4(a), DuoTok yields superior vocal reconstruction fidelity across all objective metrics. Given the limitations of speech-centric metrics for music, the accompaniment evaluation relies on Mel distance and is further validated by a blinded MOS study (Table 4(b)). The consistent preference for DuoTok in subjective ratings confirms that the observed objective gains translate effectively to human auditory perception.

6 Analysis

The main results show that DuoTok effectively reduces modeling uncertainty in multi-track LMs. To determine whether these gains stem from robust

Table 1: **Main comparison on the codec benchmark.** We report predictability (cnBPT), an auxiliary semantic accessibility diagnostic (MTT tagging AP/AUC), and reconstruction quality (Mel). DuoTok achieves the lowest cnBPT at 0.75 kbps while maintaining competitive reconstruction. Speech-oriented proxies (PESQ/STOI) are deferred to the appendix. Default official configurations are used for all baselines.

Model	Metadata			Tagging		Predictability	Recon.
	Rate	Size (S)	Kbps	MTT-AP ↑	AUC ↑	cnBPT ↓	Mel ↓
<i>Reconstruction-oriented</i>							
DAC (Kumar et al., 2023)	75 Hz	8×1024	6.00	0.20	0.79	0.76	0.73
EnCodec (Défossez et al., 2022)	75 Hz	8×1024	6.00	0.18	0.76	0.71	0.78
WavTokenizer (Ji et al., 2024)	40 Hz	1×4096	0.48	0.17	0.74	0.61	1.15
<i>Semantic-oriented</i>							
SemantiCodec (Liu et al., 2024)	50 Hz	2×8192	1.30	0.32	0.88	0.54	0.98
X-Codec (Ye et al., 2024)	50 Hz	8×1024	4.00	0.32	0.87	0.56	0.91
<i>Music-oriented</i>							
X-Codec (YuE) (Yuan et al., 2025)	50 Hz	16×1024	8.00	0.32	0.87	0.63	0.90
MuCodec (LeVo) (Lei et al., 2025; Xu et al., 2024)	25 Hz	2×16384	0.70	0.26	0.84	0.50	1.37
DuoTok (Ours)	25 Hz	2×32768	0.75	0.35	0.87	0.48	0.95

Table 2: **Unconditional multi-track LM results.** We report both cnBPT and enBPT.

Model	Size	Track	Acc			cnBPT ↓	enBPT ↓
			@1	@10	@50		
X-Codec (YuE)	8×1024	Vocal	0.15	0.44	0.70	0.632	0.773
		Accomp	0.15	0.45	0.73	0.630	0.735
		Avg	-	-	-	0.631	0.754
MuCodec (LeVo)	2×16384	Vocal	0.15	0.45	0.67	0.485	0.497
		Accomp	0.15	0.41	0.64	0.517	0.536
		Avg	-	-	-	0.501	0.516
DuoTok	2×32768	Vocal	0.14	0.43	0.67	0.461	0.501
		Accomp	0.11	0.36	0.61	0.506	0.533
		Avg	-	-	-	0.483	0.516

Table 3: **Track-to-track modeling (Vocal → Accomp).** Lower cnBPT and enBPT indicate that the tokenizer structure supports effective cross-track conditioning.

Model	Size	Acc			cnBPT ↓	enBPT ↓
		@1	@10	@50		
X-Codec (YuE)	8×1024	0.15	0.46	0.73	0.593	0.691
MuCodec (LeVo)	2×16384	0.17	0.46	0.69	0.488	0.505
DuoTok	2×32768	0.13	0.41	0.66	0.464	0.489

cross-track dependencies and long-range context rather than mere local regularities, we perform a series of controlled sanity checks.

6.1 Cross-track Structural Sensitivity

To quantify the reliance on cross-track dependencies, we quantify the relative predictability cost ΔcnBPT when corrupting the conditioning track:

$$\Delta\text{cnBPT}(\%) = 100 \cdot \frac{\text{cnBPT}_{\text{Corrupt}} - \text{cnBPT}_{\text{Clean}}}{\text{cnBPT}_{\text{Clean}}} \quad (8)$$

Three perturbation types are considered: **temporal shift**, **random masking**, and **uncorrelated mismatches** replacing the conditioning track with an unrelated sample.

Table 4: **Controlled decoder comparison.** (a) Objective metrics. (b) Simplified MOS study.

<i>(a) Objective metrics</i>				
Type	Codec	PESQ ↑	STOI ↑	Mel ↓
Vocal	MuCodec (LeVo)	1.28	0.35	1.39
	DuoTok	1.76	0.55	0.81
Accomp	MuCodec (LeVo)	-	-	1.85
	DuoTok	-	-	1.14
<i>(b) Subjective MOS (1-5)</i>				
Type	GT	MuCodec (LeVo)	DuoTok	
Vocal	4.61 ± 0.12	1.51 ± 0.09	3.66 ± 0.05	
Accomp	4.52 ± 0.19	1.85 ± 0.11	3.07 ± 0.12	

Fig. 3 illustrates that all perturbations significantly increase the ΔcnBPT , with mismatch yielding the largest cost. Specifically, the increase of cnBPT in DuoTok is 17.3%, substantially higher than 15.5% for MuCodec (LeVo) and 3.6% for X-Codec (YuE). Additionally, Fig. 3 shows that temporal shifts incur non-trivial predictability penalties, which saturate as the degree of misalignment increases. A similar trend is observed for random masking, where DuoTok exhibits a near-monotonic rise in ΔcnBPT proportional to the mask ratio. Overall, these perturbation tests indicate that LMs trained on DuoTok tokens are consistent with a stronger reliance on cross-track conditioning.

6.2 Context Scaling

The impact of temporal context on modeling efficiency is assessed by evaluating cnBPT across increasing context lengths. As illustrated in Fig. 4, cnBPT decreases for both DuoTok and MuCodec (LeVo), confirming the effective utilization of extended dependencies. Notably, DuoTok exhibits

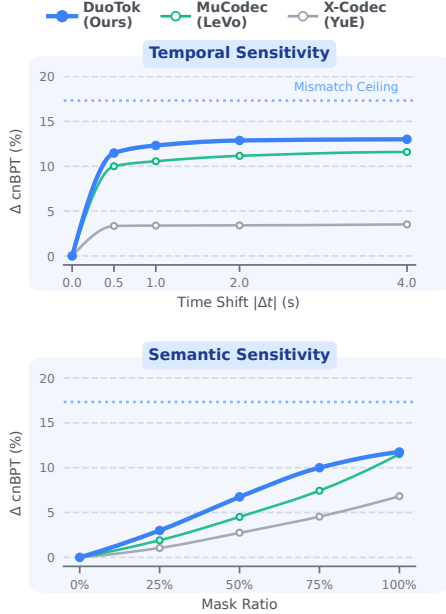


Figure 3: **Cross-track structural sensitivity.** ΔcnBPT under temporal shifts, random masking, and mismatch. DuoTok shows a larger predictability cost under correspondence-breaking corruptions.

a steeper reduction, suggesting higher context-scaling efficiency. This advantage is partially attributable to the explicit vocal-accompaniment codebook separation; in contrast, X-Codec (YuE) lacks such a multi-track structure and yields significantly lower gains from extended context.

Ablations. We ablate three tokenizer training choices that most directly affect LM predictability. Feature-replacement noise in Stage 2 is critical for modelability, raising Avg. cnBPT from 0.4832 to 0.5374 when removed, while Mel reconstruction remains essentially unchanged. Freezing the encoder before hard dual-codebook routing stabilizes discretization, and removing this step yields the largest predictability degradation, increasing Avg. cnBPT to 0.6004 and sharply lowering $\text{Acc}@k$ on both tracks. The MSS regularizer exhibits a fidelity–predictability trade-off: removing it slightly improves Avg. cnBPT but worsens Mel reconstruction on vocals. We ablate MSS in Stage 2, since MSS is inactive in Stage 3 where inputs are track-separated pseudo-stems. Full ablation results are reported in Appendix D (Tables 10 and 9).

6.3 Codebook utilization.

As a diagnostic for codebook health and to support entropy-based normalization in enBPT , we report

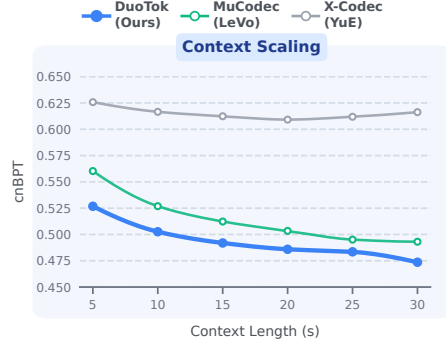


Figure 4: **Context scaling.** cnBPT decreases with longer context. DuoTok shows a steeper reduction than MuCodec (LeVo) and X-Codec (YuE).

code usage statistics in Appendix E.1 (Zhu et al., 2024). DuoTok exhibits near-full utilization and high normalized entropy on both tracks, consistent with stable use of the discrete space rather than index collapse.

7 Conclusion

We frame music tokenization as the interface between continuous waveforms and multi-track language modeling. An effective tokenizer must remain reconstructable, preserve musically meaningful semantics, and yield token sequences that are predictable under an LM, while maintaining cross-track correspondence.

We proposed DuoTok, a source-aware music tokenizer trained via staged disentanglement: semantic pretraining, structural regularization, hard dual-codebook routing, and diffusion decoding that decouples token learning from waveform synthesis.

Across standard benchmarks, DuoTok achieves a favorable predictability–fidelity trade-off, attaining the lowest codebook-normalized LM cross-entropy and the best tagging-probe AP among compared methods, while maintaining competitive reconstruction quality at low bitrate. On the held-constant dual-track LM evaluation, entropy-normalized predictability supports the same conclusion beyond codebook-size effects. Our diagnostic analyses further show larger penalties under cross-track corruption and stronger improvements with longer context, supporting the interpretation that LMs trained on DuoTok tokens exploit cross-track structure and non-local history beyond local regularities.

8 Limitations

Dependency on pseudo-stems and separation artifacts. Our dual-track pipeline relies on pseudo-stems from off-the-shelf separation, which introduces potential artifact leakage. While we mitigate this in training—specifically through MSS mask distillation in Stage 2 and frozen encoding in Stage 3—the tokenizer remains susceptible to these artifacts during inference. Consequently, separation errors from external models are unavoidable and may affect both token representation and downstream generation.

Scope of disentanglement. We adopt the vocal–accompaniment split as a minimal yet widely validated factorization for songs. Recent multi-track generation systems and their paired tokenization pipelines predominantly operate in this dual-track setting, enabling synchronized modeling and track-conditioned control (Yuan et al., 2025; Lei et al., 2025, 2024; Xu et al., 2024). This choice also aligns with our evaluation: established baselines and LM backbones are readily available in the dual-track paradigm, allowing controlled and fair comparisons.

In principle, extending disentanglement to finer-grained stems (e.g., drums or bass) could further sharpen semantic boundaries and improve editability by making each stream more source-specific. However, scaling staged routing beyond two tracks remains challenging in practice: instrument-level pseudo-stems are less reliably defined and more error-prone, and the routing–quantization design must scale without degrading codebook utilization or cross-track consistency. We therefore focus on dual-track vocal–accompaniment structure, and leave hierarchical and N -track extensions to future work.

Coverage of LM evaluation. To ensure a controlled comparison, our multi-track LM evaluation focuses on music-oriented tokenizers within dual-track pipelines (Yuan et al., 2025; Lei et al., 2025). This specific scope is necessary because general audio codecs often lack matched multi-track LM architectures and conditioning interfaces. Furthermore, we acknowledge that token rate is still a substantial factor that constrains effective context length under fixed computational budgets.

Scope of end-to-end generation. We focus on intrinsic properties of the token space, namely predictability and reconstruction fidelity, which in-

fluence downstream LM performance. End-to-end lyric-conditioned generation introduces additional components that can dominate perceptual outcomes, including alignment quality, long-horizon planning, sampling, and rendering. A fair perceptual comparison would require training large lyric-conditioned multi-track LMs to convergence under matched data mixtures and compute, which is costly and sensitive to recipe choices.

Track-wise asymmetry. Vocal tokens achieve lower cnBPT than accompaniment tokens, likely related to the strong text-aligned supervision from the ASR head. In contrast, the accompaniment track lacks such high-level symbolic priors. Future work could bridge this gap by incorporating structure-aware supervision for instruments, such as beat-tracking or symbolic cues, to harmonize representation quality across tracks.

9 Ethical Considerations

We train DuoTok exclusively on publicly available corpora and follow their respective licenses/terms of use; we do not redistribute the underlying audio. Our tokenizer is an interface for downstream generative modeling and, like other components in this pipeline, may contribute to misuse such as copyright infringement or unauthorized imitation when paired with a renderer; we therefore recommend rights-aware data governance and deployment safeguards in downstream systems. For subjective listening tests (MOS), participants provided ratings only; we did not collect personally identifying information and no monetary compensation was provided.

References

- Andrea Agostinelli, Timo I. Denk, Zalán Borsos, Jesse Engel, Mauro Verzetti, Antoine Caillon, Qingqing Huang, Aren Jansen, Adam Roberts, Marco Tagliasacchi, Matt Sharifi, Neil Zeghidour, and Christian Frank. 2023. *Musiclm: Generating music from text*. *Preprint*, arXiv:2301.11325.
- Alexei Baevski, Henry Zhou, Abdelrahman Mohamed, and Michael Auli. 2020. *wav2vec 2.0: A framework for self-supervised learning of speech representations*. *arXiv preprint arXiv:2006.11477*.
- Max Bain, Jaesung Huh, Tengda Han, and Andrew Senior. 2023. *Whisperx: Time-accurate speech transcription of long-form audio*. *INTERSPEECH 2023*.
- Ilja Baumann, Dominik Wagner, Korbinian Riedhammer, and Tobias Bocklet. 2025. *Optimized*

- self-supervised training with best-rq for speech recognition. *arXiv preprint arXiv:2501.16131*.
- Dmitry Bogdanov, Minz Won, Philip Tovstogan, Alastair Porter, and Xavier Serra. 2019. [The mtg-jamendo dataset for automatic music tagging](#). In *Machine Learning for Music Discovery Workshop, International Conference on Machine Learning (ICML 2019)*, Long Beach, CA, United States.
- Sanyuan Chen, Chengyi Wang, Zhe Jin, Yu Wu, Jian Xue, Shujie Liu, Zhuo Chen, Jinyu Li, and Yifan Gong. 2021. [Wavlm: Large-scale self-supervised pre-training for full stack speech processing](#). *arXiv preprint arXiv:2110.13900*.
- Michaël Defferrard, Kirell Benzi, Pierre Vandergheynst, and Xavier Bresson. 2017. [Fma: A dataset for music analysis](#). *Preprint*, arXiv:1612.01840.
- Alexandre Défossez, Nicolas Usunier, Léon Bottou, and Francis Bach. 2019. [Music source separation in the waveform domain](#). *arXiv preprint arXiv:1911.13254*.
- Jacob Devlin, Ming-Wei Chang, Kenton Lee, and Kristina Toutanova. 2018. [BERT: pre-training of deep bidirectional transformers for language understanding](#). *CoRR*, abs/1810.04805.
- Alexandre Défossez, Jade Copet, Gabriel Synnaeve, and Yossi Adi. 2022. [High fidelity neural audio compression](#). *Preprint*, arXiv:2210.13438.
- Alexandre Défossez, Laurent Mazaré, Manu Orsini, Amélie Royer, Patrick Pérez, Hervé Jégou, Edouard Grave, and Neil Zeghidour. 2024. [Moshi: a speech-text foundation model for real-time dialogue](#). *Preprint*, arXiv:2410.00037.
- Zach Evans, Julian D. Parker, CJ Carr, Zack Zukowski, Josiah Taylor, and Jordi Pons. 2024. [Stable audio open](#). *Preprint*, arXiv:2407.14358.
- Eduardo Fonseca, Xavier Favory, Jordi Pons, Frederic Font, and Xavier Serra. 2022. [Fsd50k: An open dataset of human-labeled sound events](#). *IEEE/ACM Transactions on Audio, Speech, and Language Processing*, 30:829–852.
- Zhifu Gao, Zerui Li, Jiaming Wang, Haoneng Luo, Xian Shi, Mengzhe Chen, Yabin Li, Lingyun Zuo, Zhihao Du, Zhangyu Xiao, and Shiliang Zhang. 2023. [Funasr: A fundamental end-to-end speech recognition toolkit](#). In *INTERSPEECH*.
- Yitian Gong, Lu Hou, Sibofeng, Biao Zhang, Zhiyong Wu, and Helen Meng. 2024. [Xy-tokenizer: Mitigating the semantic-acoustic conflict in low-bitrate speech codecs](#). *arXiv preprint arXiv:2404.04522*.
- Wei-Ning Hsu, Benjamin Bolte, Yao-Hua Sung, and James Glass. 2021. [Hubert: Self-supervised speech representation learning by masked prediction of hidden units](#). *arXiv preprint arXiv:2106.07447*.
- Shengpeng Ji, Ziyue Jiang, Wen Wang, Yifu Chen, Minghui Fang, Yi Ren, Zhiyong Wu, and Yuxuan Wang. 2024. [Wavtokenizer: an efficient acoustic discrete codec tokenizer for audio language modeling](#). *arXiv preprint arXiv:2408.16532*.
- Rithesh Kumar, Prem Seetharaman, Alejandro Luebs, Ishaan Kumar, and Kundan Kumar. 2023. [High-fidelity audio compression with improved rvqgan](#). In *Advances in Neural Information Processing Systems (NeurIPS)*. NeurIPS 2023.
- Luca A. Lanzetta, Florian Grötschla, Emil Funke, and Roger Wattenhofer. 2023. [Disco-10m: A large-scale music dataset](#). *arXiv preprint arXiv:2306.13512*.
- Edith Law, Kris West, Michael I Mandel, Mert Bay, and J Stephen Downie. 2009. Evaluation of algorithms using games: The case of music tagging. In *ISMIR*, pages 387–392.
- Shun Lei, Yaoxun Xu, Zhiwei Lin, Huaicheng Zhang, Wei Tan, Hangting Chen, Jianwei Yu, Yixuan Zhang, Chenyu Yang, Haina Zhu, Shuai Wang, Zhiyong Wu, and Dong Yu. 2025. [Levo: High-quality song generation with multi-preference alignment](#). *Preprint*, arXiv:2506.07520.
- Shun Lei, Yixuan Zhou, Boshi Tang, Max W. Y. Lam, Feng Liu, Hangyu Liu, Jingcheng Wu, Shiyin Kang, Zhiyong Wu, and Helen Meng. 2024. [Songcreator: Lyrics-based universal song generation](#). *Preprint*, arXiv:2409.06029.
- Haohe Liu, Xuenan Xu, Yi Yuan, Mengyue Wu, Wenwu Wang, and Mark D. Plumbley. 2024. [Semanticcodec: An ultra low bitrate semantic audio codec for general sound](#). *arXiv preprint arXiv:2405.00233*.
- Zihan Liu, Shuangrui Ding, Zhixiong Zhang, Xiaoyi Dong, Pan Zhang, Yuhang Zang, Yuhang Cao, Dahua Lin, and Jiaqi Wang. 2025. [Songgen: A single stage auto-regressive transformer for text-to-song generation](#). *Preprint*, arXiv:2502.13128.
- Wei-Tsung Lu, Ju-Chiang Wang, Qiuqiang Kong, and Yun-Ning Hung. 2023. [Music source separation with band-split rope transformer](#). *arXiv preprint arXiv:2309.02612*.
- William Peebles and Saining Xie. 2022. [Scalable diffusion models with transformers](#). *arXiv preprint arXiv:2212.09748*.
- Zafar Rafii, Antoine Liutkus, Fabian-Robert Stöter, Stylianos Ioannis Mimilakis, and Rachel Bittner. 2019. [Musdb18-hq - an uncompressed version of musdb18](#).
- Robin Rombach, Andreas Blattmann, Dominik Lorenz, Patrick Esser, and Björn Ommer. 2022. [High-resolution image synthesis with latent diffusion models](#). In *Proceedings of the IEEE/CVF Conference on Computer Vision and Pattern Recognition*, pages 10684–10695.

- Yakun Song, Jiawei Chen, Xiaobin Zhuang, Chenpeng Du, Ziyang Ma, Jian Wu, Jian Cong, Dongya Jia, Zhuo Chen, Yuping Wang, Yuxuan Wang, and Xie Chen. 2025. [Magicodec: Simple masked gaussian-injected codec for high-fidelity reconstruction and generation](#). *arXiv preprint arXiv:2506.00385*.
- Kangdi Wang, Zhiyue Wu, Dinghao Zhou, Rui Lin, Junyu Dai, and Tao Jiang. 2025a. [Back to ear: Perceptually driven high fidelity music reconstruction](#). *Preprint*, arXiv:2509.14912.
- Lu Wang, Hao Chen, Siyu Wu, Zhiyue Wu, Hao Zhou, Chengfeng Zhang, Ting Wang, and Haodi Zhang. 2025b. [Audiocodecbench: A comprehensive benchmark for audio codec evaluation](#). *Preprint*, arXiv:2509.02349.
- Zihao Wang, Shuyu Li, Tao Zhang, Qi Wang, Pengfei Yu, Jinyang Luo, Yan Liu, Ming Xi, and Kejun Zhang. 2024. [Muchin: A chinese colloquial description benchmark for evaluating language models in the field of music](#). *Preprint*, arXiv:2402.09871.
- Yaoxun Xu, Hangting Chen, Jianwei Yu, Wei Tan, Shun Lei, Zhiwei Lin, Chuang Wang, Weiwei Xia, Jian Luan, Renhong Liu, Zhiyong Wu, Wei Wang, Dan Su, Yuxuan Wang, and Haizhou Li. 2024. [Mucodec: Ultra low-bitrate music codec](#). *arXiv preprint arXiv:2409.13216*.
- Chenyu Yang, Shuai Wang, Hangting Chen, Wei Tan, Jianwei Yu, and Haizhou Li. 2025. [Songbloom: Coherent song generation via interleaved autoregressive sketching and diffusion refinement](#). *arXiv preprint arXiv:2506.07634*.
- Zhen Ye, Peiwen Sun, Jiahe Lei, Jiawen Wu, Yi Huang, Qinfei Chen, Yang Zhang, and Yi Shan. 2024. [Codec does matter: Exploring the semantic shortcoming of codec for audio language model](#). *arXiv preprint arXiv:2408.17175*.
- Ruibin Yuan, Hanfeng Lin, Shuyue Guo, Ge Zhang, Jiahao Pan, Yongyi Zang, Haohe Liu, Yiming Liang, Wenye Ma, Xingjian Du, Xinrun Du, Zhen Ye, Tianyu Zheng, Zhengxuan Jiang, Yinghao Ma, Minghao Liu, Zeyue Tian, Ziya Zhou, Liumeng Xue, and 39 others. 2025. [Yue: Scaling open foundation models for long-form music generation](#). *Preprint*, arXiv:2503.08638.
- Neil Zeghidour, Alejandro Luebs, Ahmed Omran, Jan Skoglund, and Marco Tagliasacchi. 2021. [Soundstream: An end-to-end neural audio codec](#). *arXiv preprint arXiv:2107.03312*.
- Xin Zhang, Dong Zhang, Shimin Li, Yaqian Zhou, and Xipeng Qiu. 2024. [Spechtokenizer: Unified speech tokenizer for speech large language models](#). *Preprint*, arXiv:2308.16692.
- Yongxin Zhu, Bocheng Li, Yifei Xin, and Linli Xu. 2024. [Addressing representation collapse in vector quantized models with one linear layer](#). *arXiv preprint arXiv:2411.02038*.

A Predictability Metrics

A.1 Codebook-normalized BPT is a fair, dimensionless measure

A dimensionless ratio. Let $x \in \{1, \dots, S\}$ denote a token from a codebook of size S , with data distribution $p(x)$ and model predictive distribution $q(x)$. The token-level cross-entropy in bits is

$$H(p, q) = \mathbb{E}_{x \sim p}[-\log_2 q(x)], \quad (9)$$

which is exactly the reported bits per token (BPT). Consider the uniform predictor $u(x) = 1/S$. For any p ,

$$H(p, u) = \mathbb{E}_{x \sim p}[-\log_2(1/S)] = \log_2 S. \quad (10)$$

We define codebook-normalized BPT as

$$\text{cnBPT} = \frac{H(p, q)}{\log_2 S} = \frac{H(p, q)}{H(p, u)}. \quad (11)$$

This ratio is dimensionless and removes the trivial scaling with the vocabulary size. In particular, $\text{cnBPT} = 1$ corresponds to uniform prediction, and smaller values indicate stronger predictability.

Coding interpretation. $\log_2 S$ is the code length of an ideal fixed-length index over a codebook of size S . $H(p, q)$ is the expected code length induced by the language model under teacher forcing. Therefore, cnBPT measures *coding efficiency* relative to the fixed-length baseline, yielding a tokenizer-agnostic notion of learnability that is comparable across codebook sizes.

Multi-codebook setting. We consider K codebooks per time step. Let S_k be the size of codebook k , and let

$$\ell_{t,k} = -\log_2 q_{t,k}(x_{t,k} \mid \text{context}) \quad (12)$$

denote the per-token loss in bits at time t . The reported BPT averages over time and codebooks,

$$\text{BPT} = \frac{1}{TK} \sum_{t=1}^T \sum_{k=1}^K \ell_{t,k}. \quad (13)$$

The corresponding fixed-length baseline is the mean index length per codebook,

$$\text{BPT}_{\text{fixed}} = \frac{1}{K} \sum_{k=1}^K \log_2 S_k, \quad (14)$$

yielding the general normalization

$$\text{cnBPT} = \frac{\text{BPT}}{\text{BPT}_{\text{fixed}}}. \quad (15)$$

When all codebooks share the same size $S_k = S$, Eq. (15) reduces to $\text{cnBPT} = \text{BPT}/\log_2 S$. Finally, cnBPT normalizes only the codebook size. It does not absorb token rate or the number of codebooks per step, which directly affect bitrate and are therefore reported separately.

A.2 Transparency of multi-track LM predictability metrics

To make predictability comparisons inspectable, we report raw BPT in addition to cnBPT . We further report entropy-normalized BPT (enBPT), which normalizes cross-entropy by the empirical unigram code entropy on the evaluation set. This removes the uniform-code approximation implicit in dividing by $\log_2 S$ and helps disambiguate effects due to codebook size.

From cnBPT to enBPT . Recall that $\text{BPT} = H(p, q)$ and $\text{cnBPT} = H(p, q)/\log_2 S$. Let $H(p)$ denote the empirical unigram entropy of the code distribution. We define

$$\text{enBPT} = \frac{H(p, q)}{H(p)} = \frac{\text{BPT}}{H(p)}. \quad (16)$$

Using the normalized entropy statistic reported in Appendix E, $H_{\text{norm}} = H(p)/\log_2 S$, we obtain

$$\text{enBPT} = \frac{\text{cnBPT}}{H_{\text{norm}}}. \quad (17)$$

When the code distribution is close to uniform, $H_{\text{norm}} \approx 1$ and cnBPT is a close proxy of enBPT .

Invariance of relative changes. For a fixed evaluation setting, H_{norm} depends only on the empirical code distribution and is constant with respect to the LM. Therefore, any relative predictability cost reported with cnBPT is unchanged when expressed with enBPT , e.g., $\Delta \text{enBPT}(\%) = \Delta \text{cnBPT}(\%)$.

Scope. We report transparency results only for *music-oriented tokenizers* that are paired with strong music language models and naturally support the dual-track protocol. Specifically, we include YuE, MuCodec from LeVo, and DuoTok. Other codecs are omitted because they are not released with advanced music LMs under the same dual-track evaluation protocol.

Table 5: Transparency of predictability metrics for multi-track LMs. We report cnBPT, BPT, and enBPT, where enBPT is computed using empirical unigram code entropy statistics in Appendix E. S is the single-codebook size.

Model	Size S	$\log_2 S$	Uncond. Vocal			Uncond. Accomp			Cond. V→A		
			cnBPT	BPT	enBPT	cnBPT	BPT	enBPT	cnBPT	BPT	enBPT
X-Codec (YuE)	1,024	10	0.632	6.315	0.773	0.630	6.303	0.735	0.593	5.928	0.691
MuCodec (LeVo)	16,384	14	0.485	6.793	0.497	0.517	7.242	0.536	0.488	6.836	0.505
DuoTok	32,768	15	0.461	6.911	0.501	0.506	7.586	0.533	0.464	6.962	0.489

A.3 Frame Rate and Codebook-Normalized Rate (cnBPS)

While cnBPT (Appendix A.1) normalizes predictability *per token*, tokenizers can differ substantially in how many tokens they emit per second. To make this interface difference explicit and quantify the modeling burden per unit time, we formalize the tokenizer-LM interface and derive a rate-aware metric.

Interface and rate accounting. We characterize a discrete interface by a **frame rate** f (Hz) and K discrete indices emitted per frame. For a single stream, the **token emission rate** (tokens/s) is

$$\tau = fK. \quad (18)$$

A tokenizer may use heterogeneous codebooks with sizes $\{S_k\}_{k=1}^K$. Under fixed-length indices, codebook k requires $\log_2 S_k$ bits per token, so the fixed-length **index bitrate** (bits/s) is

$$b = f \sum_{k=1}^K \log_2 S_k. \quad (19)$$

When all codebooks share a size $S_k = S$, this simplifies to $b = \tau \log_2 S$. For multi-stream tokenizers (e.g., vocal and accompaniment), we report total rates by summation:

$$\tau_{\text{tot}} = \sum_r \tau_r, \quad b_{\text{tot}} = \sum_r b_r, \quad (20)$$

where r indexes streams (tracks).

Codebook-normalized rate (cnBPS). Since cnBPT is a per-token quantity, two tokenizers with identical cnBPT may impose different per-second modeling burdens if their token emission rates τ differ. We define the per-second cross-entropy rate as $\text{BPS} = \tau \cdot \text{BPT}$ (bits/s). Recall that $\text{cnBPT} = \text{BPT} / \text{BPT}_{\text{fixed}}$, where the fixed-length index cost per token is

$$\text{BPT}_{\text{fixed}} = \frac{1}{K} \sum_{k=1}^K \log_2 S_k \quad (\text{Eq. 14}). \quad (21)$$

We then define codebook-normalized bits per second as

$$\text{cnBPS} = \tau \cdot \text{cnBPT} = \frac{\text{BPS}}{\text{BPT}_{\text{fixed}}}. \quad (22)$$

This preserves the codebook-size normalization of cnBPT while explicitly accounting for the linear scaling of per-second burden with token emission rate. We emphasize that cnBPS has units of s^{-1} and measures the rate-normalized modeling burden under fixed-length index coding. (i.e., not the bitrate of an entropy-coded stream).

Multi-stream additivity. For multiple streams r , the total normalized burden is the sum over streams:

$$\text{cnBPS}_{\text{tot}} = \sum_r \tau_r \cdot \text{cnBPT}_r. \quad (23)$$

Equivalently, letting $\text{cnBPT}_{\text{avg}} = \frac{\sum_r \tau_r \text{cnBPT}_r}{\sum_r \tau_r}$, we have $\text{cnBPS}_{\text{tot}} = \tau_{\text{tot}} \text{cnBPT}_{\text{avg}}$.

A.4 Benchmarking Modeling Efficiency

Table 6 reports interface metadata (frame rate f , size $K \times S$, token emission rate τ) and the resulting per-second predictability. cnBPT values align with the main benchmark, while cnBPS is defined in Eq. (22) and aggregated across streams via Eq. (23).

Implications. The comparison highlights a trade-off between per-token learnability and emission rate. A high-rate codec may achieve competitive cnBPT yet still impose a substantially larger per-second burden due to its larger τ (Eq. (22)). By achieving a low $\text{cnBPS}_{\text{tot}}$, DuoTok indicates not only predictable tokens but also an interface that is structurally efficient for long-context sequence modeling.

B Evaluation Protocol Details

B.1 Multi-track LM evaluation protocol

This section provides protocol details for the multi-track LM evaluation in Sec. 4.2, including multi-

Table 6: **Tokenizer interface summary and per-second predictability.** We report **frame rate** f (Hz), interface size $K \times S$, token emission rate $\tau = fK$ (Eq. (18)), and fixed-length *index* bitrate b (Eq. (19)). For dual-track tokenizers with shared codebook sizes, $K \times S$ counts codebooks across both tracks; per-track K is reflected in the per-track τ . Total rates sum over tracks (Eq. (20)). We compute total per-second predictability as $\text{cnBPS}_{\text{tot}} = \sum_r \tau_r \text{cnBPT}_r$ (Eq. (23)). cnBPS is a normalized rate (not an entropy-coded bitrate).

Model	Interface			Token emission rate		Index bitrate		Predictability	
	Stream	f (Hz)	Size $K \times S$	τ (track)	τ (total)	b (track)	b (total)	cnBPT	cnBPS _{tot}
<i>Reconstruction-oriented</i>									
DAC	mix	75	8×1024	600	600	6.00	6.00	0.76	456.0
EnCodec	mix	75	8×1024	600	600	6.00	6.00	0.71	426.0
WavTokenizer	mix	40	1×4096	40	40	0.48	0.48	0.61	24.4
<i>Semantic-oriented</i>									
SemantiCodec	mix	50	2×8192	100	100	1.30	1.30	0.54	54.0
X-Codec	mix	50	8×1024	400	400	4.00	4.00	0.56	224.0
<i>Music-oriented</i>									
X-Codec (YuE)	vocal+accomp	50	16×1024	400	800	4.00	8.00	0.63	504.0
MuCodec (LeVo)	vocal+accomp	25	2×16384	25	50	0.35	0.70	0.50	25.0
DuoTok (Ours)	vocal+accomp	25	2×32768	25	50	0.38	0.75	0.48	24.0

codebook input formatting, loss computation, and auxiliary metrics.

B.1.1 LM backbone and held-constant settings

We use the same LM backbone and training budget across tokenizers. The backbone is Qwen2-1B. Across all tokenizers in the LM evaluation, we hold constant: (i) optimizer and learning-rate schedule, (ii) total optimization steps, and (iii) audio context duration (30 s). All token sequences are derived from the same underlying audio segments to ensure a controlled comparison.

B.1.2 Multi-codebook input representation

Tokenizers may output indices from multiple codebooks at each time step. We map them into a single LM input vector by embedding each codebook index with a dedicated embedding table, concatenating the embeddings, and projecting to the LM hidden dimension D . Let $x_{t,k}$ denote the token index from codebook k at time t . The LM input $\mathbf{u}_t \in \mathbb{R}^D$ is:

$$\mathbf{u}_t = \mathbf{W}_{\text{in}} [\mathbf{E}_1(x_{t,1}) \oplus \dots \oplus \mathbf{E}_K(x_{t,K})], \quad (24)$$

where $\mathbf{E}_k(\cdot)$ is the embedding lookup for codebook k , \oplus denotes concatenation, and \mathbf{W}_{in} is a learned projection.

B.1.3 Parallel unconditional prediction

In the unconditional setting, we jointly model vocal and accompaniment streams and predict all codebooks in parallel. We use one prediction head per

codebook and minimize the teacher-forced cross-entropy loss, averaged uniformly over time steps and codebooks. For a tokenizer with K_v vocal codebooks and K_i accompaniment codebooks, this protocol uses $K_v + K_i$ parallel heads.

B.1.4 Track-to-track conditional generation

In the track-to-track setting, we predict a target track conditioned on a source track. We provide the LM with the full 30 s conditioning-track sequence and the first 2 s of the target track as a prefix, then predict the remaining target tokens. Losses are computed only on the target-track tokens.

B.1.5 Auxiliary interpretability metric

We additionally report top- k next-token accuracy ($\text{Acc}@k$) as an auxiliary interpretability metric. $\text{Acc}@k$ is the fraction of positions where the ground-truth token appears in the model’s top- k predictions under teacher forcing. We treat $\text{Acc}@k$ as a diagnostic and do not use it for model selection.

B.2 Tagging probe protocol

We follow AudioCodecBench (Wang et al., 2025b) to assess whether discrete codes preserve high-level musical attributes, using the MagnaTagATune (MTT) Top-50 tag set (Law et al., 2009).

Probe input (post-quantization only). To restrict the probe to information available from discrete tokens, we use only post-quantization code embeddings (i.e., codebook vectors) and do not access any continuous encoder states. We freeze the entire codec and optimize only the probe.

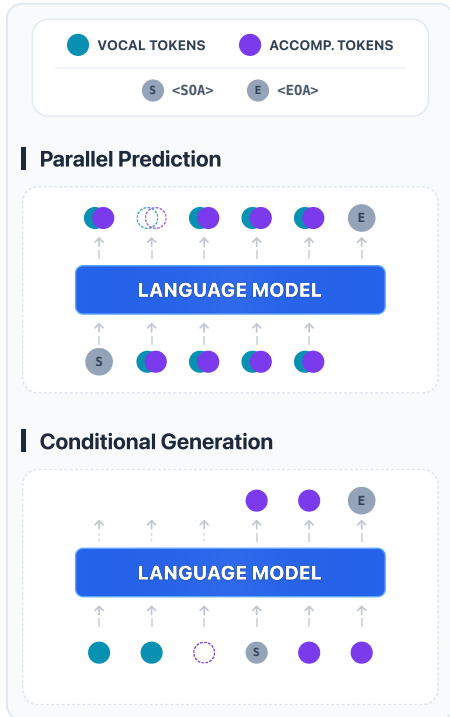


Figure 5: Multi-track LM protocols: parallel prediction and track-to-track conditioning.

Probe architecture. We feed embedding sequences into a lightweight Conformer initialized from scratch, followed by a linear classification head. We use the same probe architecture across tokenizers for a controlled comparison.

Evaluation. We report Average Precision (AP) and Area Under the ROC Curve (AUC) on the test set as defined in Sec. 4.3.

B.3 Reconstruction evaluation protocol

Standard reconstruction. For each tokenizer, we run its standard encoding/decoding pipeline on fixed 30 s audio segments and compute objective reconstruction metrics as described in Sec. 4.3. All clips use the same evaluation splits and loudness normalization.

B.3.1 Controlled decoder protocol

To reduce decoder confounds, we perform a controlled reconstruction comparison between DuoTok and MuCodec (Xu et al., 2024) by training an identical latent diffusion decoder on frozen codebook embeddings to predict continuous autoencoder latents. We predict 50 Hz latents with a 64-dimensional bottleneck following standard latent-diffusion audio pipelines (Wang et al., 2025a; Evans et al., 2024).

Matched-decoder setup. For each tokenizer, we freeze the pre-trained codebook embeddings and train the same latent diffusion decoder to predict 50 Hz autoencoder latents. We train for 276k steps for each tokenizer variant under the same optimization settings. This matched-decoder protocol probes reconstructability while holding decoder capacity fixed.

MOS assessment. We further assess perceptual quality via a blinded MOS test with $N = 12$ clips and 10 ratings per clip on a 1–5 scale, including ground-truth (GT) anchors. MOS instructions and presentation protocol are provided in Appendix B.4.

B.4 MOS protocol

We conduct a small-scale MOS study for the controlled reconstruction comparison in Table 4. Raters score the perceptual quality of each audio clip on a 5-point Likert scale (higher is better) using the following guidelines:

- **5 (Excellent):** Imperceptible difference from natural recordings.
- **4 (Good):** Minor artifacts that are perceptible but not intrusive.
- **3 (Fair):** Noticeable artifacts that degrade the listening experience but remain acceptable.
- **2 (Poor):** Intrusive artifacts or discontinuities that are unpleasant to listen to.
- **1 (Bad):** Dominated by severe artifacts or noise.

All stimuli are loudness-normalized and presented with anonymized labels in randomized order via an online form. Raters evaluate each clip independently and may replay samples as needed.

C Data and Training Details

C.1 Datasets and splits

We train DuoTok using only public corpora. Stage 1 utilizes a broad collection including LibriTTS, FSD50K, FMA, DISCO-10M, MuChin, and Jamendo (Fonseca et al., 2022; Defferrard et al., 2017; Lanzend"orfer et al., 2023; Wang et al., 2024; Bogdanov et al., 2019). In Stage 2 and Stage 3, we exclude LibriTTS and other strictly non-lyric datasets to concentrate on musical and vocal-centric content. When official train/validation/test

splits are provided, we follow them. Otherwise, we create non-overlapping splits by track identity to avoid content leakage.

C.2 Preprocessing and pseudo-stem generation

To enable dual-track modeling without proprietary multitrack data, we synthesize pseudo-stems using Demucs, producing vocal and accompaniment stems (Défossez et al., 2019). Given the pseudo-stems, we construct four types of training samples:

- **Full mix:** the original mixture audio (no separation).
- **Lyric-active vocal:** vocal segments restricted to lyric-active regions, avoiding long silent spans.
- **Lyric-aligned accompaniment:** accompaniment segments aligned to the same lyric-active regions.
- **Instrumental-only accompaniment:** accompaniment segments without vocals (e.g., intros, outros, bridges, and instrumental solos).

For lyric-annotated tracks, we apply lyric-aware segmentation and split audio into 5–30 s clips based on sentence boundaries to preserve semantic coherence.

C.3 Training hyperparameters and sampling ratios

Training samples. We use mixture-dominant sampling in Stage 2 and stem-dominant sampling in Stage 3 to balance global structure and source specialization under the dual codebooks.

ASR supervision coverage. We distinguish *lyric-available* batches from *ASR-active* batches. In Stage 2, lyric-available batches account for 5/7 of steps under the 4:1:1:1 mixture, while the ASR loss is applied only when the vocal stream corresponds to lyric-active vocal batches. In Stage 3, lyric availability is exactly 50% under the 5:4:1 mixture, again computing ASR only on lyric-active vocal batches.

Optimization. Across stages, we use AdamW with a warmup–cosine learning-rate schedule. Stage 1 follows the BEST-RQ recipe, while Stage 2 and Stage 3 perform multi-task adaptation and discrete code learning.

Table 7 summarizes training hyperparameters for Stage 1–Stage 3. We also report stage-specific loss weights and data mixture ratios for reproducibility.

C.4 Stage 4: per-track latent diffusion decoder training

Overview. In Stage 4, we train separate latent diffusion decoders for vocals and accompaniment (no parameter sharing). Each decoder operates on fixed 30 s segments and predicts continuous autoencoder latents at 50 Hz with a 64-dimensional bottleneck (Wang et al., 2025a). We use the open-source implementation of `stable-audio-tools` and the official, publicly available EAR-VAE encoder (Wang et al., 2025a). This ensures that our renderer setup is fully reproducible using off-the-shelf community components.

Optimization. We use AdamW with $\beta = (0.8, 0.99)$, $\epsilon = 10^{-5}$, and weight decay 0.01. We use a warmup schedule with peak learning rate 2×10^{-4} , 2k warmup steps, and cosine decay to a final learning-rate ratio of 0.5. The global batch size is 120.

Inference setting. Unless otherwise stated, we use 50 denoising steps for all diffusion decoders. For controlled-decoder comparisons (Appendix B.3.1), we use checkpoints trained for 276k steps to keep the matched-decoder evaluation consistent across tokenizers.

C.5 Model configurations

This section summarizes architecture configurations of DuoTok, including encoder/quantizer settings (codebook sizes and counts), auxiliary heads used in Stage 2, and the per-track diffusion decoder used in Stage 4. Unless otherwise stated, we follow the default configurations of released checkpoints for baselines.

C.6 Compute and implementation details

We report implementation settings that affect reproducibility, including hardware, effective batch sizes, and key training details (e.g., mixed precision and gradient accumulation when applicable).

Table 7: Training hyperparameters for DuoTok in Stage 1–Stage 3.

Hyperparameter	Stage 1 (SSL)	Stage 2 (multi-task)	Stage 3 (SimVQ)
Optimizer	AdamW	AdamW	AdamW
(β_1, β_2)	(0.9, 0.96)	(0.9, 0.96)	(0.9, 0.96)
Weight decay	0.1	0.1	0.1
LR scheduler	Warmup–cosine	Warmup–cosine	Warmup–cosine
Peak learning rate	3×10^{-4}	1×10^{-4}	1×10^{-4}
Warmup steps	5k	3k	3k
Cosine cycle length	50k	80k	30k
Training steps	3M	100k	100k
Global batch size	1,920	448	1,280
<i>Stage-specific settings</i>			
Objectives / loss weights	SSL objective only	$\lambda_{\text{ASR}} : \lambda_{\text{Mel}} : \lambda_{\text{Chr}} : \lambda_{\text{MSS}}$ = 0.5 : 1 : 1 : 1	$\lambda_{\text{Mel}} : \lambda_{\text{Chr}} : \lambda_{\text{VQ}}$ = 1 : 1 : 1
Gaussian replacement (p, σ)	—	(0.2, 1.0)	—
Data mixture ratio	—	full : vocal : accomp : instr. = 4 : 1 : 1 : 1	vocal : accomp : instr. = 5 : 4 : 1

Table 8: Stage-4 decoder training configuration.

Hyperparameter	Vocal decoder	Accomp decoder
Target latent (rate, dim)	50 Hz, 64-d	50 Hz, 64-d
Backbone	stable-audio-tools	stable-audio-tools
Parameters	~400M	~400M
Segment length	30 s	30 s
Optimizer	AdamW	AdamW
(β_1, β_2)	(0.8, 0.99)	(0.8, 0.99)
Weight decay	0.01	0.01
LR scheduler	Warmup–cosine	Warmup–cosine
Peak learning rate	2×10^{-4}	2×10^{-4}
Warm-up steps	2k	2k
Final LR ratio	0.5	0.5
Global batch size	120	120
<i>Evaluation-facing settings</i>		
Inference steps	50	50
Controlled-decoder checkpoint	276k	276k

D Ablations

We ablate three design choices in tokenizer training: (i) the MSS objective used in Stage 2, (ii) Gaussian replacement corruption in Stage 2 multi-task training, and (iii) stage-wise optimization when introducing hard dual-codebook routing in Stage 3. The **w/o Enc Freeze** variant does not freeze the encoder in Stage 3, and instead jointly fine-tunes the encoder and quantizers under the same training budget. All other settings follow Appendix C.

D.1 Reconstruction ablation

Table 9 reports reconstruction fidelity.

- **w/o MSS:** Mel distance increases on both tracks, suggesting MSS helps preserve source-specific spectral detail.

Table 9: Reconstruction ablation on Mel L1 (\downarrow). Mean \pm std. **w/o Enc Freeze** jointly fine-tunes the encoder and quantizers in Stage 3.

Tokenizer	Mel distance \downarrow	
	Vocal	Accomp
DuoTok	0.240 \pm 0.026	0.219 \pm 0.030
w/o MSS	0.249 \pm 0.021	0.223 \pm 0.021
w/o Noise	0.248 \pm 0.018	0.219 \pm 0.020
w/o Enc Freeze	0.250 \pm 0.023	0.210 \pm 0.029

- **w/o Noise:** Reconstruction is largely unchanged, consistent with noise primarily targeting robustness for sequence modeling.
- **w/o Enc Freeze:** Vocal reconstruction worsens, while accompaniment improves. This indicates that jointly adapting the encoder and

Table 10: Unconditional LM ablation. $\text{Acc}@k$ (\uparrow) and cnBPT (\downarrow). We train the same LM on tokens from each tokenizer variant and report results on vocals and accompaniment. Avg. cnBPT is the mean over the two tracks.

Tokenizer	Vocal					Accomp					Avg.
	Acc@1	Acc@5	Acc@10	Acc@50	cnBPT	Acc@1	Acc@5	Acc@10	Acc@50	cnBPT	cnBPT
DuoTok	0.1433	0.3308	0.4345	0.6660	0.4607	0.1077	0.2656	0.3596	0.6117	0.5057	0.4832
w/o MSS	0.1585	0.3553	0.4594	0.6853	0.4469	0.1026	0.2546	0.3466	0.5988	0.5129	0.4800
w/o Noise	0.1087	0.2622	0.3530	0.5745	0.5148	0.0794	0.2046	0.2838	0.5163	0.5599	0.5374
w/o Enc Freeze	0.0542	0.1552	0.2229	0.4342	0.6079	0.0551	0.1555	0.2259	0.4502	0.5929	0.6004

quantizers can bias capacity allocation across tracks.

D.2 Predictability ablation

Table 10 shows that Gaussian replacement corruption is important for predictability: removing it increases Avg. cnBPT from 0.4832 to 0.5374. Removing MSS slightly improves cnBPT but worsens reconstruction in Table 9, reflecting a fidelity–predictability trade-off.

Crucially, **w/o Enc Freeze** in Stage 3 yields the worst predictability, increasing Avg. cnBPT to 0.6004 and sharply degrading $\text{Acc}@k$ on both tracks. This supports the staged disentanglement design: once hard dual-codebook routing is introduced, freezing the encoder stabilizes the representation that the quantizers discretize. Without this stage-wise separation, the encoder can drift to favor reconstruction-specific variability, producing higher-entropy codes that are substantially harder for the LM to model.

E Codebook Health Diagnostics

E.1 Codebook utilization and normalized entropy

We report code usage statistics on the validation set as a diagnostic for codebook stability. These statistics also provide the empirical code entropy needed to compute enBPT in Appendix A.2.

For each codebook, we compute:

- **Utilization:** the fraction of codebook entries that appear at least once.
- **Normalized entropy (H_{norm}):** the empirical unigram entropy of the code distribution divided by $\log_2 S$, where S is the codebook size.

Figure 6 visualizes utilization and H_{norm} . Table 11 summarizes the same diagnostics for the music-oriented tokenizers used in the dual-track LM setting.

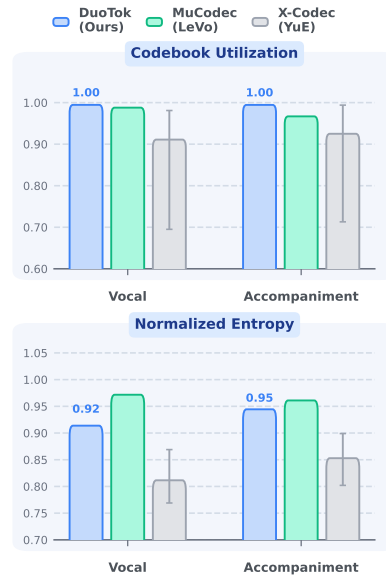


Figure 6: Codebook usage diagnostics on the validation set: utilization and normalized entropy.

Table 11: Codebook health diagnostics on the validation set.

Codec	Track	Util.	H_{norm}
DuoTok	Vocal	0.9996	0.9188
	Accomp	0.9995	0.9494
MuCodec (LeVo)	Vocal	0.9929	0.9767
	Accomp	0.9719	0.9660
X-Codec (YuE)	Vocal	0.9162	0.8165
	Accomp	0.9299	0.8579